Poly(ethylene terephthalate) (PET) degradation during the Zn catalysed transesterification with dibutyl maleate functionalized polyolefins

Maria-Beatrice Coltelli [a,*], Sabrina Bianchi [b], Mauro Aglietto [b]

[a] *Centro Italiano Packaging and Dipartimento di Chimica e Chimica Industriale, via Risorgimento 35, 56126 Pisa, Italy*
[b] *Dipartimento di Chimica e Chimica Industriale, via Risorgimento 35, 56126 Pisa, Italy*

Abstract

The chemical reactions occurring during the melt blending between a dibutyl maleate functionalized polyolefin (POF) and poly(ethylene terephthalate) (PET) in the presence of $Zn(OOCCH_3)_2 \cdot 2H_2O$ were studied as a function of blending conditions, such as the preliminary drying of PET, the presence of a nitrogen flow during blending and the time of blending. The selective extraction of POF/PET 30/70 by weight blends to remove unreacted PET and the determination of its molecular weight by viscosimetric measurements allowed to evaluate both the grafting points' number and the molecular weight of PET. In this way the impact of degradation of PET onto its grafting by transesterification onto POF was investigated. The examined blending conditions were shown to affect both PET degradation and POF–PET copolymer formation. In order to correlate data about macromolecular and morphological structure with the final properties of the blends, differential scanning calorimetry (DSC), scanning electron microscopy (SEM) and tensile tests were also carried out.
© 2007 Elsevier Ltd. All rights reserved.

Keywords: Polyester degradation; PET/polyolefin blends; Reactive blending

1. Introduction

During processing PET undergoes hydrolytic, thermal and thermo-oxidative chain scission [1–3].

The hydrolytic degradation consists of the random breakage of the PET chain by water molecules and it results in the formation of a hydroxyl and a carboxylic group for each breakage. Zimmerman and Kim [4] showed the effect of terminal COOH groups' concentration on the hydrolysis kinetics and in particular they demonstrated the autocatalytic mechanism of the hydrolysis, more recently observed also in solid state polymerization of PET [5] and in hydrolysis of poly-(butylene terephthalate) (PBT) [6]. Al-AbdulRazzak and Jabarin [1] studied the effect of temperature and moisture content in the hydrolysis of PET during melt processing.

They showed that the hydrolysis is a very fast reaction and that its rate was proportional to the water concentration and to the concentration of carboxylic groups. In some cases the hydrolytic stability of polyesters was improved by reducing the terminal carboxylic acid groups' concentration [1,5,6]. Many evidences were reported in the literature confirming the reversibility of hydrolysis and suggested the possibility of driving it by controlling the concentration of water [7] and the processing parameters [8].

The thermal degradation processes were also widely investigated, but there is still some controversy about the assessment of a radical or ionic mechanism [9]. Anyway the final products of thermal degradation are generally considered cyclic oligomers, terminal carboxylic and vinyl groups and acetic aldehyde [10–12].

Goodman and Nesbitt [13] investigated the PET degradation as a consequence of the cyclic oligomer formation in the molten polyesters and considered that they could be formed by both the nucleophilic attack of hydroxyl groups

---

on the polyester chain and the direct interchange transesterification involving only ester groups. Ha and Choun [14] successively suggested that the concentration of cyclic oligomers formed in the melt followed a linear dependence versus the starting concentration of hydroxyl terminal groups. Hence the terminal OH groups favour the formation of cyclic oligomers improving the reduction of PET molecular weight.

Bothelo et al. [3] studied the thermal degradation of PET using low molecular weight model compounds. They proposed a radical mechanism starting from the breakage of the ester C−O linkage. The oxygen radical thus formed was able to give hydrogen abstraction with formation of acid groups. The carbon radicals were involved in termination by coupling, thus resulting in butylene terephthalate units. Recent studies [15] carried out by thermal analysis−infrared spectroscopy (TA−FT-IR) suggested the formation of acetic aldehyde, CO_2 and condensed aromatic rings by a free radical path during thermal degradation. On the other side the formation of COOH and vinyl groups was also explained by a six-centre electrocyclic mechanism that results in the random breakage of an ester bond of the chain [3].

The reactions of thermo-oxidative degradation are additionally complicated by the oxygen action. It was suggested that the process starts with the formation of a hydroperoxide at the methylene group, followed by homolytic chain scission of the C−O bond [3]. Bikiaris and Karayannidis evidenced that the carboxyl terminal groups have a promoting activity in thermo-oxidative degradation of PET [16]. Moreover temperature and diethylene glycol content can affect deeply the thermo-oxidative degradation. In particular the methylene in α position with respect to the ester linkage was reported to undergo hydrogen abstraction in the presence of *t*-butoxy radicals [17].

Paci and La Mantia [18] evidenced a strict dependence of the operative conditions on the degradation of the recycled PET. In fact the presence of a flow of nitrogen during blending can induce an increase in PET molecular weight, as evidenced by torque measurements and molecular weight determinations. The result was attributed to the absence of the oxidative degradation path in the presence of the nitrogen flow. More recently the presence of oxygen was reported to yield degradation of dried and molten PET at atmospheric pressure, whereas it gave crosslinking when the partial pressure of oxygen was reduced below 600 Pa [8].

The presence of metal was reported to affect the thermal properties [19] and the degradation behaviour [4] of PET, as it is reported to be involved in thermal degradation pathways. In fact the metal complexation to the adjacent carbonyl group can affect the electronic distribution at the carbon involved in the electrocyclic hydrogen transfer of thermal degradation [20] thus favouring chain scission. Metal catalysts are thus used also for the high temperature degradation of PET wastes [21].

During the blending with other polymers, such as polyolefin, PET could undergo a similar degradation leading to not easily predictable final properties, as phase morphology and final properties depend on structural and rheological characteristics of blend components [22,23]. In many cases blends of polyolefin and PET are compatibilized by introducing a polymer bearing groups reactive towards PET terminal groups [24−28]. In this case degradation affects the type and concentration of terminal groups which can influence the extent of compatibilization reaction occurring at the interface between the two immiscible phases [29,30], determining the final structure of the formed polyolefin−PET copolymer. With the aim of investigating these aspects, PET scraps were blended in different operative conditions with dibutyl maleate functionalized polyethylene in order to evaluate the effect of blending conditions on reactive compatibilization and phase morphology development. The transesterification between the two different macromolecular species was also studied in the presence of zinc acetate.

2. Experimental part

2.1. Materials

Polyolefin material is 85/15 by weight blend of Engage 8003 ethylene−octene copolymer (30% by weight of comonomer content, MFR = 1 g/10 min at 190 °C and 2.16 kg, density = 0.886 g/cm^3) and Riblene (Polimeri Europa) is a low density polyethylene (LDPE, MFR = 10 dg/min, $M_w = 233,500$; Id = 2.03). LDPE was added to the ethylene−octene copolymer to reduce the melt viscosity of the polyolefin phase, thus promoting the assessment of a low diameter dispersed phase in PET based blends [23]. The mixture was functionalized in a semi-industrial batch mixer in the melt with dibutyl maleate (DBM) in the presence of dicumyl peroxide (DCP) as radical initiator. The material was minced and purified by continuous extraction with boiling acetone for 16 h in order to remove low molecular weight compounds, such as unreacted DBM and peroxide decomposition products. This polyolefin material showed a functionalization degree FD = 0.8% by moles determined by FT-IR method [31] and a molecular weight $M_w = 188,500$ (Id = 3.6) as obtained by SEC measurements (Water GPC-V instrument, trichlorobenzene, 145 °C).

Post-consumer PET colourless flakes named SERI-L/AN with intrinsic viscosity = 0.774 dl/g (phenol/tetrachloroethane 60/40 v/v) corresponding to $M_w = 45,300$ and $M_n = 22,900$ [32] were purchased from Se.Ri.Plast. $Zn(OOCCH_3)_2 \cdot 2H_2O$ was a Carlo Erba commercial product.

1,1,1,3,3,3-Hexafluoro-2-propanol and methane dichloride were purchased from Aldrich.

2.2. Reactive blending

Blends were prepared in a 50 ml Brabender discontinuous mixer at 250 °C with a blade rate of 80 rpm. To allow an easy and secure feeding of the mixer the polymeric materials and additives were introduced at 40 rpm. After 2 min, the velocity was increased linearly to 80 rpm till 3 min and kept constant till the end of the experiment, at 10 min. After mixing the recovered material was cooled at room temperature.

2.3. Characterization

A small quantity (0.6 g) of compression moulded and finely minced blends has been extracted with an 80/20 v/v solution of 1,1,1,3,3,3-hexafluoro-2-propanol (HFIP)/methane dichloride (DCM) for 4 h. The obtained dispersions have been filtered and washed with fresh solvent on the filter. After the removal of solvent by vacuum the residual and extracted fractions have been weighed and characterized by FT-IR.

IR spectra were measured with a Perkin–Elmer 1330 Fourier transform infrared spectrometer on compression moulded films.

Intrinsic viscosity of extracted PET was determined in phenol/tetrachloroethane 60/40 by weight solution (ASTM D 4603-96) by using a capillary viscosimeter.

A Jeol JSM model T-300 was used for scanning electron microscopy (SEM) and cryogenically broken surfaces were examined after sputtering with gold.

Differential scanning calorimetry (DSC) was performed by using a DSC 822e – Mettler Toledo with a Star^e software version 6.10. An aluminium standard crucible with 10–20 mg of sample was employed. A first heating scan from 25 to 280 °C at 10 °C/min was followed by cooling down to 25 °C at 20 °C/min and by a second heating up to 280 °C at 10 °C/min under a nitrogen atmosphere.

Tensile tests were carried out by using an INSTRON 5564 dynamometer. The specimens were prepared onto compression moulded films, conditioned by following the ASTM 1708-93 normative and tested at a rate of 10 mm/min.

3. Results and discussion

3.1. Effect of operative conditions on PET flakes' blending

PET was processed for 10 min in different operative conditions, that is simply closing the mixer (−), flowing nitrogen during blending (N2), previously drying the PET (d) or they both (N2d) (Table 1). Moreover the effect of $Zn(OOCCH_3)_2 \cdot 2H_2O$ (C blends) was evaluated in all the operative conditions and two blends with a higher percentage of $Zn(OOCCH_3)_2 \cdot 2H_2O$ were also prepared (CAN2 and CAN2d runs).

Table 1
PET/metal derivative mixtures: experimental conditions and final torque values

Blends	N$_2$ flowing	PET drying	C^a (% wt)	Final torque (N m)
PET−	No	No	−	4.3
PETd	No	Yes	−	5.5
PETN2	Yes	No	−	9.8
PETN2d	Yes	Yes	−	10.8
PETC−	No	No	0.06	1.9
PETCd	No	Yes	0.06	3.8
PETCN2	Yes	No	0.06	9
PETCN2d	Yes	Yes	0.06	11.3
PETCAN2	Yes	No	0.6	5.2
PETCAN2d	Yes	Yes	0.6	6.7

^{a} 0.06% and 0.6% by weight correspond to 5.4% and 54% by moles of PET macromolecules, respectively.

The torque values increased about 5 N m in the presence of a nitrogen flow (Fig. 1a) in agreement with Paci's results [10]. The presence of water in PET may affect furthermore the torque value and a decrease of about 1 N m was observed comparing dried PET runs with not dried PET ones.

The thermo-oxidation was probably responsible for the slightly continuous decrease of torque observed in the PET and PETd runs, while the hydrolytic degradation, being a very fast reaction [1], significantly affected the first part of the same curves. The operative conditions affected more torque values when $Zn(OOCCH_3)_2 \cdot 2H_2O$ was added to the PET, as the difference between the final torque values of PETC and PETCN2d (Fig. 1a) was larger than between PET and PETN2d (Fig. 1b). The value of the difference ΔTorqueC between final torque for runs obtained in the absence and presence of $Zn(OOCCH_3)_2 \cdot 2H_2O$, respectively, in identical conditions was calculated. Moreover the presence of $Zn(OOCCH_3)_2 \cdot 2H_2O$ resulted in the decrease of torque in each condition, with the exception of N2d (Fig. 2). The decrease of ΔTorqueC for dried runs with respect to not dried ones can be easily explained by considering that the removal of water limits hydrolytic degradation catalysed by C. The presence of a difference in torque value for N2 runs is thus explainable on the basis of the catalytic activity towards hydrolytic degradation of PET. In N2d conditions the presence of the Zn derivative leads to the increase of torque (negative ΔTorqueC value), as chain extension due to transesterification prevails onto degradation. Anyway the difference in ΔTorqueC for d and N2d (and also − and N2) runs can be explained only if $Zn(OOCCH_3)_2 \cdot 2H_2O$ takes part in the thermo-oxidative degradation mechanism. Hence C is involved in hydrolytic degradation, thermo-oxidative degradation and transesterification and its contribution to torque decrease was 1.3, 2.2 and −0.5 N m, respectively.

If the content of C added to PET was increased (PETCAN2 and PETCAN2d runs, Table 1) a more extensive torque drop was observed due to the chain terminator feature of the metal derivative. In fact its acetate ligands can give nucleophilic substitution onto the polyester backbone. This undesired reactivity not only causes the decrease of the PET molecular weight but also makes it less reactive, because of the replacement of terminal hydroxyl groups with more stable acetate groups.

The DSC thermogram of PETN2d showed a double melting peak as that obtained for PET, processed without drying and in the absence of nitrogen flow. PET having a lower molecular weight usually crystallizes at higher temperature during cooling and more rapidly [33]. But in this case secondary crystallization prevails. Hence the shape differences in the thermograms can be attributed to the enhancement of the primary crystallization for the PETN2d, the melting peak of which is reported to be at higher temperature [34] (Fig. 3).

3.2. Effect of operative conditions on reactive compatibilization in PET/polyethylene 70/30 by weight blends

Some 70/30 PET/PO reference blends (A series) were prepared in different operative conditions (Table 2). Moreover
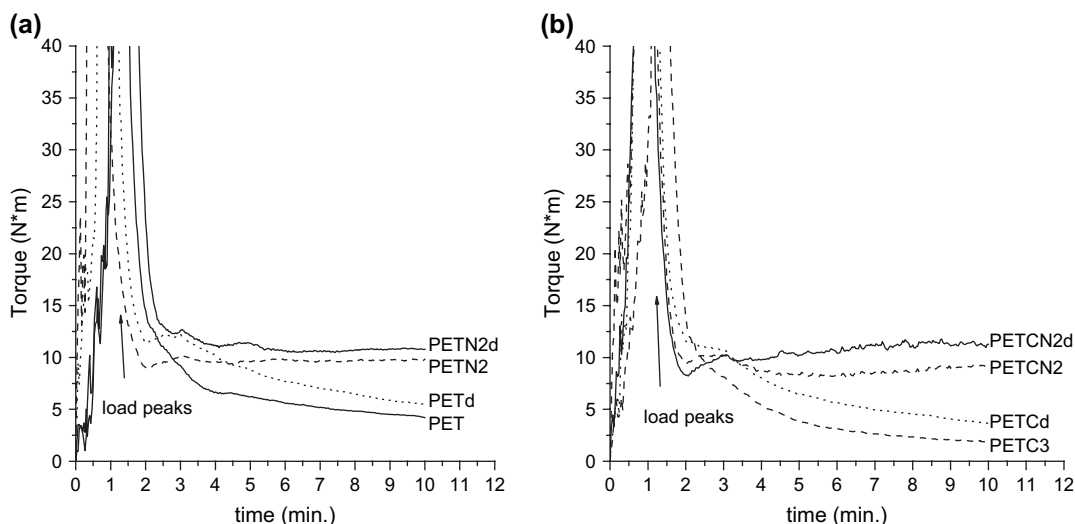
Fig. 1. Torque against time plot for PET scraps in different operative conditions in the absence (a) and presence (b) of $Zn(OOCCH_3)_2 \cdot 2H_2O$.
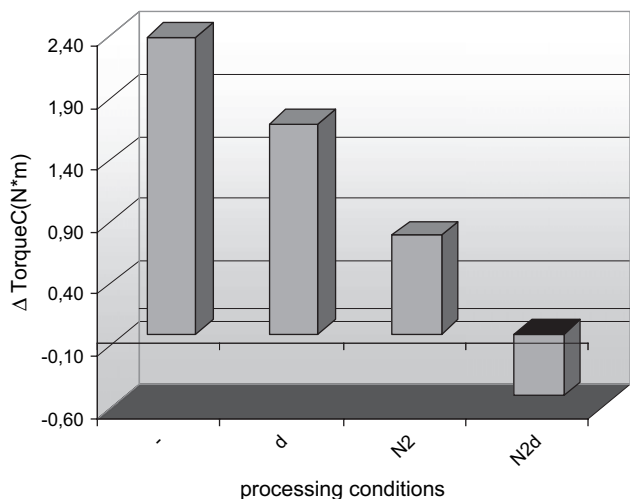

Fig. 2. Difference ΔTorqueC between final torque for runs obtained in the absence and presence of C, as a function of conditions.

70/30 PET/POF blends were prepared in the absence (B series) and presence of $Zn(OOCCH_3)_2 \cdot 2H_2O$ (C series). In the latter case the time of blending was also varied in order to evaluate its effect onto transesterification of POF with PET.

For the three different kinds of blends (A, B, C) an increase of the final torque values was observed in the following order: closing the mixing chamber (−), flowing nitrogen during blending (N2) or flowing nitrogen and drying PET (N2d). This trend agrees with the torque value results observed for neat PET runs (Table 2).

The drying of PET and the flowing of nitrogen during blending allowed to obtain for the blend CN2d a similar torque value with respect to BN2d, obtained in the absence of zinc acetate. Hence in these conditions the effect on degradation of the latter was almost overcome and a similar velocity for the PET degradation and chain extension were assumed, able to maintain almost unchanged the average molecular weight.
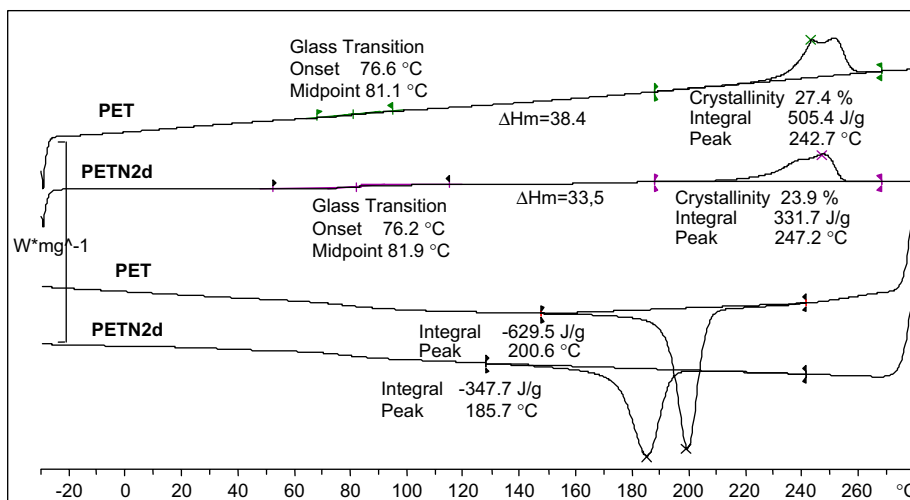

Fig. 3. DSC thermograms of PET and PETN2d: cooling (bottom) and second heating (top).

Table 2
PET/PO 70/30 blends composition, experimental conditions and final torque values

Blends	N_2 flowing	PET drying	C (% wt)	Final torque (N m)
A—[a]	No	No	—	9.1
AN2	Yes	No	—	10
AN2d	Yes	Yes	—	10.8
B—[a]	No	No	—	5.9
BN2	Yes	No	—	9.7
BN2d	Yes	Yes	—	10.2
C—[a]	No	No	0.04	5.5
CN2	Yes	No	0.04	8.9
CN2d	Yes	Yes	0.04	9.7
20—CN2d[b]	Yes	Yes	0.04	10.2
40—CN2d[b]	Yes	Yes	0.04	11.8

[a] The blend A is PET/unfunctionalized PO 70/30; the blend B is PET/POF 70/30; the blend C is PET/POF 70/30 with $Zn(OOCCH_3)_2$.
[b] 20—CN2d and 40—CN2d were prepared in N2d conditions by increasing the time of blending up to 20 and 40 min, respectively.

The C series blends were extracted with HFIP in order to remove the unreacted PET, filtered and washed. The residual fraction was compression moulded and characterized by infrared spectroscopy. The presence of grafted PET was easily revealed thanks to the intense characteristic C=O stretching band at 1727 cm^{-1}. The same analysis carried out on the residue of A blend (PET/PO blend) showed a very weak band at 1727 cm^{-1} (Fig. 4).

The area of the PET bands was calculated by a deconvolution procedure and the ratio A_1/A_2 between the area value thus calculated and the area value of a reference band allowed to determine the percentage of grafted PET (Table 3), by previously building a suitable calibration line, as described elsewhere [35]. The value of the percentage of grafted PET allowed calculating (Appendix A) the yield of the transesterification between POF and PET (Fig. 5) for each blend.

The grafting yield depends on two parameters, the number of grafting points and the PET grafted chain length, that is the grafted PET molecular weight. To evaluate if only the latter parameter had a strong effect on the yield value, the molecular
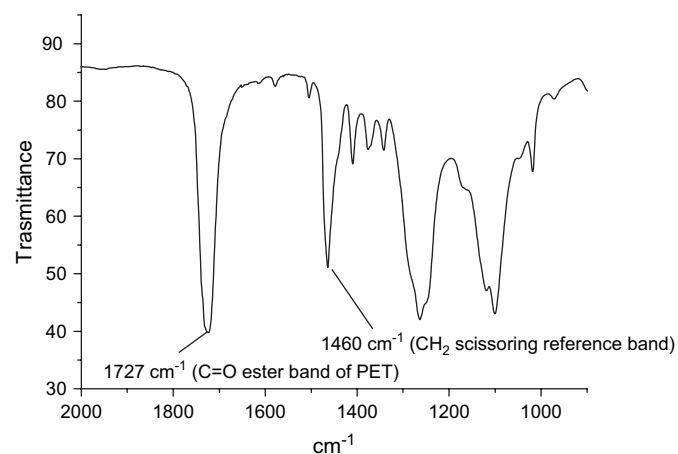

Fig. 4. FT-IR spectrum of the sample CN2d after the removal of unreacted PET by selective extraction.

Table 3
PET grafting yield as determined by selective extraction-IR spectroscopy method [35]

Blends	Residual fraction (% wt)	A_1/A_2	s_m[a]	Grafted PET in the residue (% wt)	$S_{\%PET}$[b]	PET grafting yield
A	33	0.3	0.06	2	1	0.9
B	20	0.7	0.04	5	0.9	1.4
C	26	2.7	0.5	19	4	7.4
CN2	23	1.9	0.02	14	1	4.5
CN2d	45	3.7	0.2	26	2	17.1
20—CN2d	52	4.3	0.1	30	2	22.81
40—CN2d	51	3.5	0.3	24	3	17.61

[a] s_m is the standard deviation of A_1/A_2 values.
[b] $S_{\%PET}$ is the standard deviation of the % wt of PET in the residue (see Appendix A).
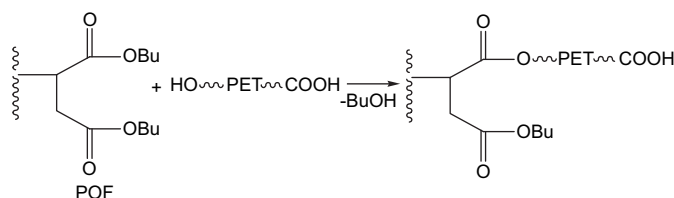

Fig. 5. Transesterification between POF (dibutyl maleate functionalized polyolefin) and PET.

weight of extracted PET fraction was determined by viscosimetric measurements [1]. Then, by assuming that the molecular weight of grafted chains was the same as unreacted PET chains, the number of grafting points was calculated (Table 4).

Both the number of grafting points and the yield with respect to DBS grafted groups were affected by processing conditions. The yield was calculated by assuming the reaction of one DBS group with one PET macromolecule. The last calculations reported in Table 4 showed that the increase of the yield is not only due to the increase of molecular weight but also due to a better efficiency of the interfacial process (Figs. 6 and 7).

The results of both grafting point number calculations and intrinsic viscosity measurements (Fig. 8) can be explained considering the different mechanisms reported in the literature about the hydrolytic, thermal and thermo-oxidative degradation. In fact in thermo-oxidative conditions (C blend) the presence of radicals, which can be formed on the functionalized polyolefin and on the PET chain, may give a copolymer

Table 4
Grafting point number and yield of DBS groups' reaction

Blends	Intrinsic viscosity	M_n	Grafting point number (mol/µg)	Yield of DBS groups reaction[a] (% by moles)
C	0.46	12,600	5.9	7.1
CN2	0.54	15,900	2.8	3.4
CN2d	0.58	17,700	9.6	11.6
20—CN2d	0.54	15,900	9.9	17.3
40—CN2d	0.52	15,100	7.9	14.2

[a] The yield was calculated by the following formula: Yield = (% moles of grafting points on POF)/$FD_{POF} \times 100$.
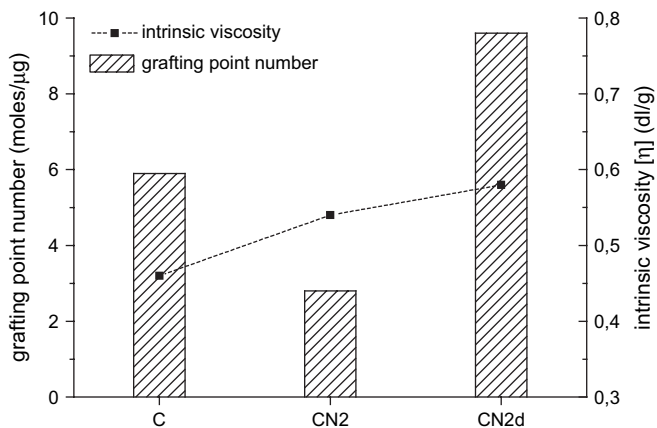
Fig. 6. Grafting points' number and intrinsic viscosity values obtained for POF/PET blends in the presence of $Zn(OOCCH_3)_2 \cdot 2H_2O$ by changing operative conditions (C = closing the chamber; CN2 = flowing nitrogen; CN2d = flowing nitrogen and previously drying PET).

Fig. 8. PET grafting points' number and intrinsic viscosity of the unreacted PET against mixing time.

through a radical coupling reaction. The removal of oxygen during blending (CN2 blend) made less effective this kind of mechanism giving a decreased PET grafting yield. In fact in this condition only the transesterification of POF with PET can give the polyolefin–PET copolymer, while the hydrolytic degradation of PET, catalysed by zinc acetate, is still occurring. When water was also removed (CN2d blend) the yield

of the latter reaction increased, as the Zn activity as transesterification catalyst was improved [36].

The blends were characterized by SEM to study the phase morphology development. The reference PO/PET blends showed in any case low adhesion between the phases. The blends obtained with a nitrogen flow showed a lower dispersed phase diameter, as a consequence of the higher viscosity of the
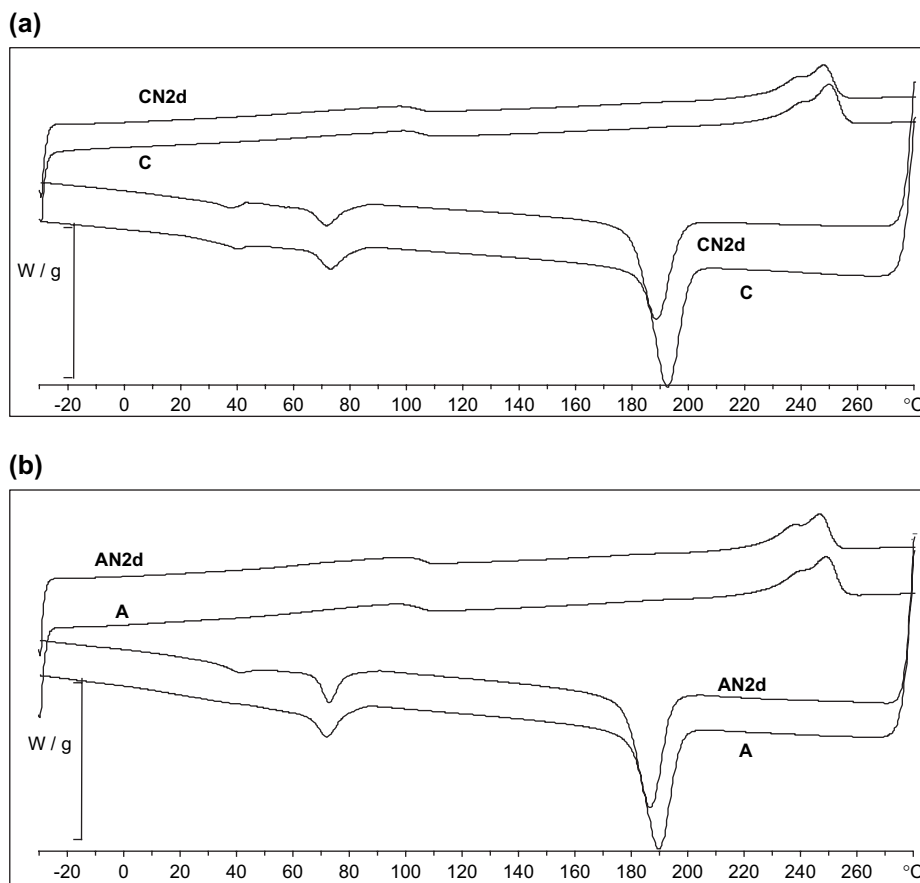
Fig. 7. DSC cooling and heating thermograms obtained for C and CN2d blends (a) and A and AN2d blends (b).

PET phase. A similar trend was observed for every row of Table 5. The level of adhesion was markedly improved in every column passing from the first to the second row.
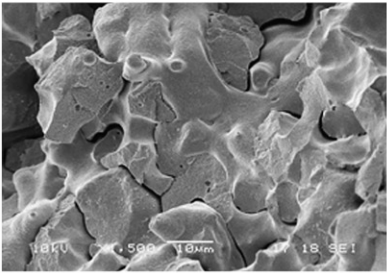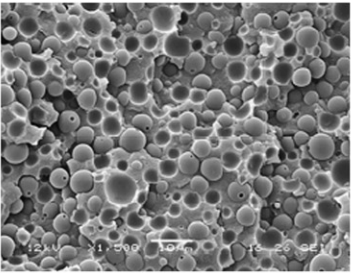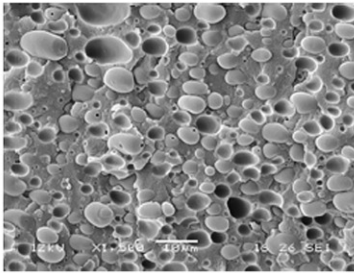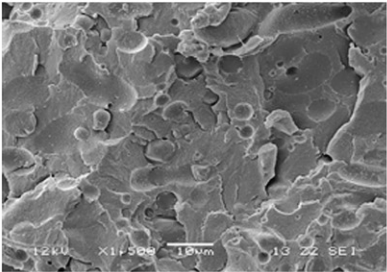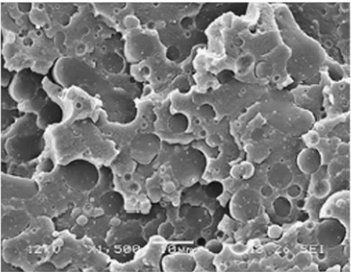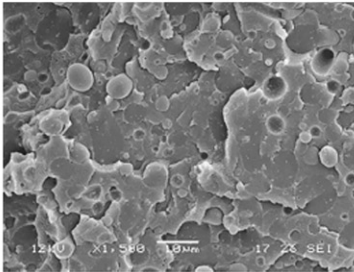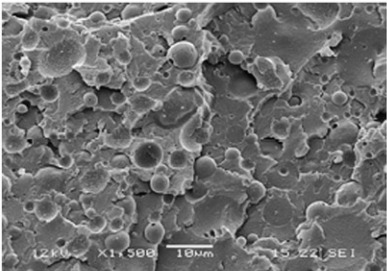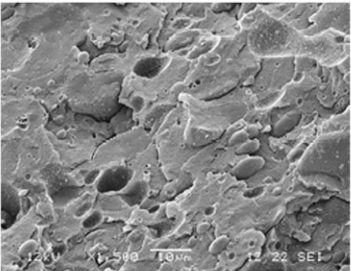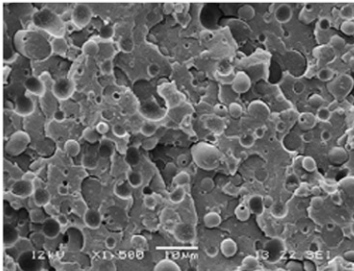
The morphologic properties of the third row blends are quite in agreement with the grafting point number results. In fact the CN2 blend phase morphology is slightly coarser than the other blends.

The comparison of the DSC cooling and heating thermograms obtained for the reference blend A and for the catalysed system C in different conditions showed a similar trend (Fig. 9). The thermal characteristics are reported in Table 6. An increase of PET T_c and $-\Delta H_c$ was observed for blends obtained in N2d conditions compared to blends obtained by simply closing the mixer, independently of the different polyethylene components and the presence of the metal derivative. Hence these variations were due to the effect of processing conditions on PET molecular weight.

The effect of mixing time on the transesterification reaction was also studied by preparing blends at 10, 20 and 40 min as mixing time (CN2d, 20—CN2d, 40—CN2d, respectively, Table 2). The final torque value increased with the blending time. The PET grafting yield (Table 4) was improved by adopting a 20 min mixing time, while a mixing time of 40 min gave a lower grafting yield, despite the higher torque value. The

Table 5
SEM micrographs of PET/polyethylene reference blends (A), PET—POF blends (B) and PET—POF blends with $Zn(OOCCH_3)_2 \cdot 2H_2O$ (C) produced in different operative conditions

10 μm

[a] _ = by closing the mixer; N2 = by flowing nitrogen; N2d = by previously drying PET and flowing nitrogen.
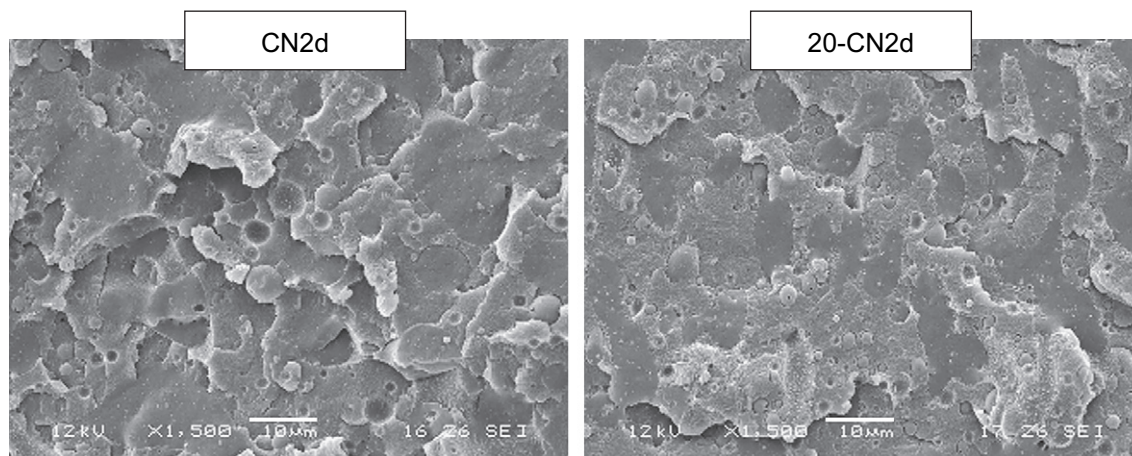
Fig. 9. SEM micrographs of the 10 min (left) and 20 min (right) blends.

Table 6
Thermal characteristics of PET in the reference blend and in compatibilized blends obtained in different conditions

	T_m (°C)	ΔH_m (J/g)	%cryst	T_c (°C)	ΔH_c (J/g)
CN2d	247.1	38.7	27.6	189.1	−37.9
C	249.1	42.3	30.2	193.1	−41.3
AN2d	246.0	39.8	27.8	187.1	−38.6
A	248.2	44.3	31.6	190.3	−41.7

intrinsic viscosity measurements obtained for the extracted PET showed a slight but continuous decrease of the molecular weight. These results disagree with the increase of torque values and can be explained on the basis of the grafted copolymer formation. At the highest mixing time the final torque value shows an increase due to a further copolymer formation. The formed copolymers have PET grafted chains with a lower molecular weight. So we can suppose that the number of

grafting points increased but the molecular weight of grafted PET chains decreased. This hypothesis is partially supported by graft point numbers' results (Table 4). In Fig. 8 this parameter was compared with the intrinsic viscosity of the extracted PET. Corresponding to the 0 mixing time the intrinsic viscosity of the pure PET was inserted in the graphic. The increase of the graft point number with the decrease of the intrinsic viscosity can be observed until 20 min.

The data of torque, graft point number and intrinsic viscosity observed for the 40 min blend are not easy to interpret. On the other hand the calculations were carried out on the basis of some approximations. In fact the PET in the blends is considered as monodispersed. Truly the PET molecular weight has a distribution curve depending on the kinetics of the reactions involving PET, so its width is a function of time. In particular an increase with mixing time of the distribution curve width can be reasonably hypothesized, by taking into account the
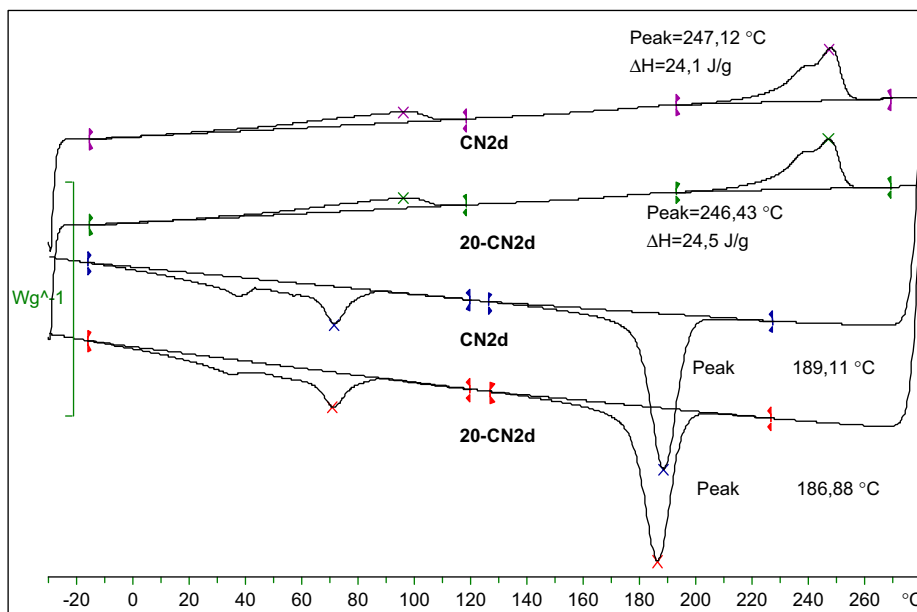

Fig. 10. DSC heating and cooling thermograms obtained for 10 and 20 min blends.

Table 7
Stress at break and elongation at break of PET and PET/poly(ethylene) blends (see Tables 1 and 2 for compositions)

Sample	Stress at break (MPa)	Elongation at break (%)
PETN2d	14.62	9.3
AN2d	13.41	10.5
BN2d	12.80	7.0
CN2d	11.81	14.3
20−CN2d	12.30	21.8

heterogeneity of the system and the presence of many reactions affecting the PET structure. Moreover the segregation of the lower molecular weight PET macromolecules in the interfacial region [37] may explain the apparent grafting point decrease for high mixing times, as they favour diffusion controlled processes.

The characteristics of SEM micrographs are in good agreement with the extraction results. The adhesion between the two phases is clearly improved in the 20 min blend with respect to the 10 min one (Fig. 9).

Moreover the DSC measurements (Fig. 10) showed a decrease of the PET crystallization temperature in the 20 min
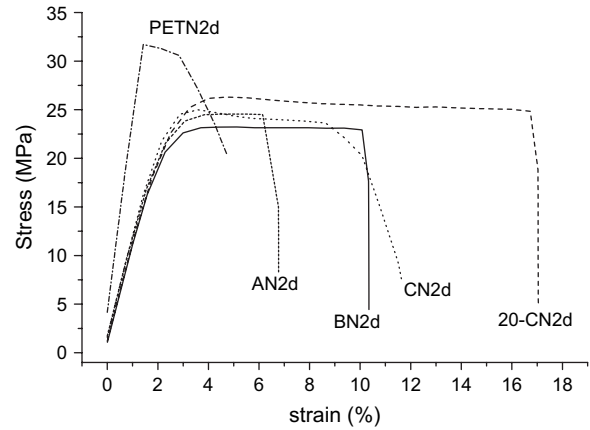

Fig. 11. Stress–strain representative curves obtained for PET and PET/POF 70/30 blends under different conditions.

blend (186.9 °C) with respect to the 10 min one (189.1 °C), in agreement with an improved compatibility of the blend.

The tensile properties of the blends were also evaluated by stress–strain tests performed on specimens drawn from compression moulded blends (Table 7).
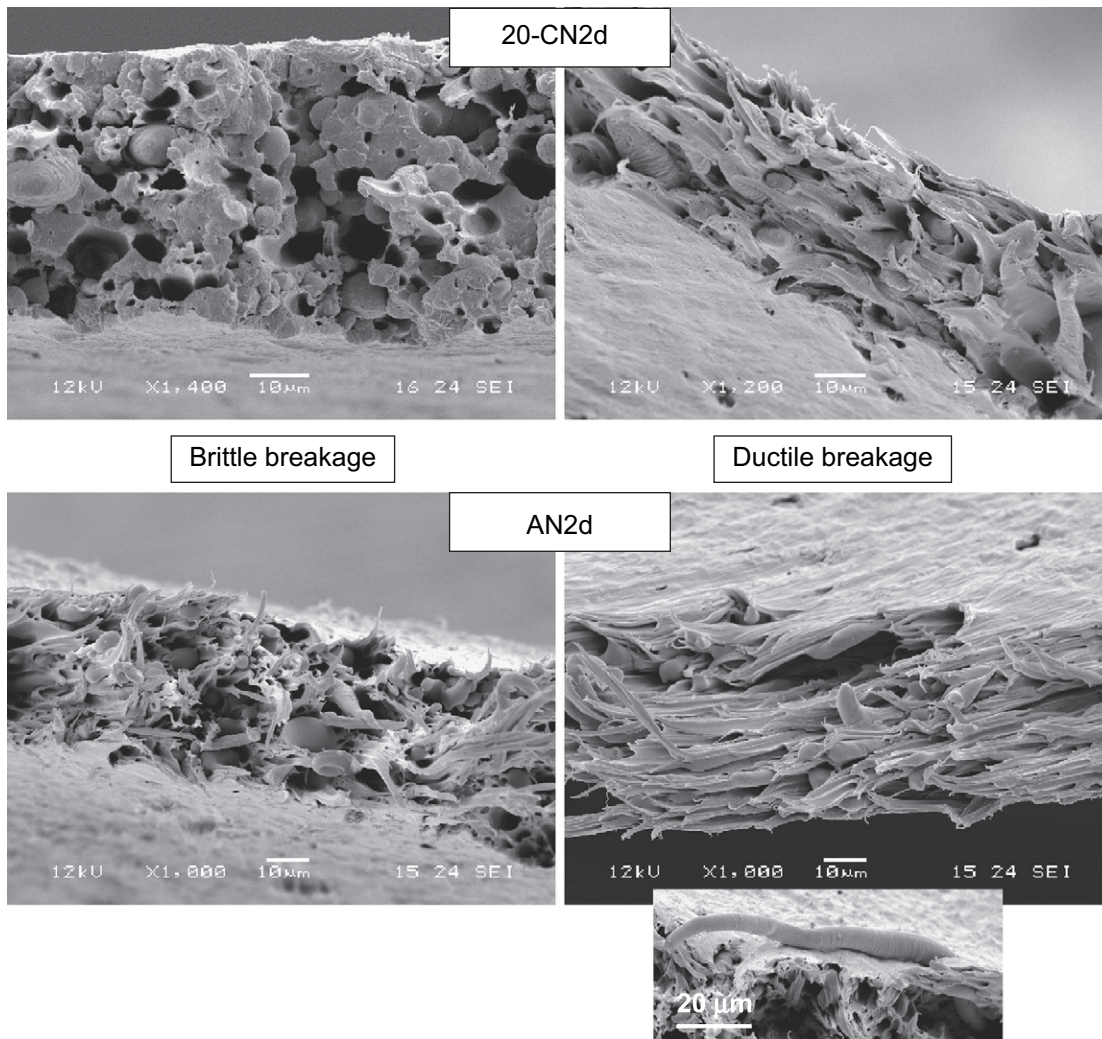

Fig. 12. SEM micrographs of the fractured surfaces of specimens broken during tensile tests. Specimens were obtained from the reactive compatibilized blend (20−CN2d, top) and reference PO/PET blend (AN2d, bottom). For each blend areas of brittle breakage (left) with areas of ductile breakage (right) were compared.

The elongation at break was higher in the blends containing the $Zn(OOCCH_3)_2$ and the 20 min blend showed the highest value. Some representative curves were reported (Fig. 11) to compare the tensile behaviour of the different blends.

The increase of the elongation at break value for the 20 min blend was reasonably due to the improved adhesion between the two phases.

The broken surface of the specimen was analysed by SEM (Fig. 12), comparing the reference blend (AN2d) with the 20 min compatibilized blend. In both the surfaces a smooth part and a rough part can be distinguished. The smooth part represents the area in which the breakage starts in a brittle way. In the rough part the fracture propagates in a ductile way and the matrix yielding can be easily observed. In the latter part a better level of adhesion between the two phases can be observed in the compatibilized 20−CN2d blend. In the surface of the latter the absence of expelled big domains is in agreement with an improved adhesion. On the contrary in the reference un-compatibilized blend AN2d many expelled large polyolefin elongated domains can be noticed.

4. Conclusions

The chemical reactions occurring during the melt blending between dibutyl maleate functionalized polyolefin (POF) and poly(ethylene terephthalate) (PET) in the presence of $Zn(OOCCH_3)_2 \cdot 2H_2O$ were studied as a function of blending conditions, such as the preliminary drying of PET, the presence of a nitrogen flow during blending and the time of blending. In particular the presence of a nitrogen flow and the preliminary removal of humidity from PET reduced PET degradation and improved the POF−PET copolymer formation in terms of graft point number. Moreover a maximum for grafting yield was observed for 20 min as blending time, probably as a consequence of the balance between the tendency to increase the grafting yield of PET onto POF and the reduction of the molecular weight of PET grafted chains by increasing the time of blending. Differential scanning calorimetry (DSC), scanning electron microscopy (SEM) and tensile measurements confirmed the trend deducted from chemical analysis, showing a good agreement between evidences about macromolecular structure and final properties of materials.

The results of this study can give some important indications, based on chemical reactivity and structure, for the preparation of blends by an innovative, sustainable and cheap process from post-consumer PET [38], with an alternative reactive blending approach, encouraging its recycling. On the basis of the present study the preparation of PET flakes based blends containing functionalized polyolefin requires the preliminary drying of flakes and the processing under nitrogen flow, as these preliminary operations much affect the occurrence of grafting between PET and functionalized polyolefin. Moreover the time of processing plays a very crucial role and it should be also optimised to achieve the right balance between PET degradation and grafting onto functionalized polyolefin by transesterification.

Appendix A

The percentage of PET grafting yield was calculated from Eq. (1):

PET grafting yield

$$= \left(\frac{\text{PET\% in the residual fraction}}{100} \times \text{residue (\% wt)} \right) \times \frac{100}{70} \tag{1}$$

The error $S_{\%PET}$ reported in Table 3 was determined considering that:

$$\%PET = a + b \times \frac{A_1}{A_2} = f\left(a, b, \frac{A_1}{A_2} \right) \tag{2}$$

where $a = 0.09 \pm 0.89$ and $b = 7.14 \pm 0.30$, as obtained by the linear fitting procedure [35].

The variance expression can be written as:

$$S_{\%PET}^2 = (df/da)^2 s_a^2 + (df/db)^2 s_b^2 + \left(df/d\frac{A_1}{A_2} \right)^2 s_m^2 \tag{3}$$

By replacing the numerical values in the equation an expression for the $S_{\%PET}$ can be obtained:

$$S_{\%PET} = \left[0.7918 + 0.0927 \times \frac{A_1^2}{A_2^2} + 50.97 \times s_m^2 \right]^{1/2} \tag{4}$$

References

[1] Al-AbdulRazzak S, Jabarin SA. Polym Int 2002;51:164.
[2] Ravidranath K, Mashelkar RA. Chem Eng Sci 1986;41:2197.
[3] Bothelho G, Queiròs A, Liberal S, Gijsman P. Polym Degrad Stab 2001;74:39.
[4] Zimmerman H, Kim NT. Polym Eng Sci 1980;20:680.
[5] Duh B. J Appl Polym Sci 2002;83:1288−304.
[6] de Gooijer JM, Scheltus M, Jansen MAG, Koning CE. Polymer 2003;44:2201−11.
[7] Guclu G, Yalcinyuva T, Ozgumus S, Orbay M. Thermochim Acta 2003;404:193−205.
[8] Assadi R, Colin X, Verdu J. Polymer 2004;45:4403−12.
[9] Montaudo G, Puglisi C, Samperi F. Polym Degrad Stab 1993;42:13.
[10] Villain FK, Coudane J, Vert M. Polym Degrad Stab 1995;49:393−7.
[11] Khemani KC. Polym Degrad Stab 2000;67:91−9.
[12] Shukla SR, Logfren EA, Jabarin SA. Polym Int 2005;54:946−55.
[13] Goodman I, Nesbitt BF. Polymer 1960;1:384.
[14] Ha WS, Choun YK. J Polym Sci 1979;17:2103.
[15] Holland BJ, Hay JN. Polymer 2002;43:1835.
[16] Bikiaris DN, Karayannidis GP. Polym Degrad Stab 1999;63:213−8.
[17] Dokolas P, Solomon DH. Polymer 2000;41:3523−9.
[18] Paci M, La Mantia FP. Polym Degrad Stab 1998;61:417.

[19] Pilati F, Toselli M, Messori M, Manzoni C, Turturro A, Gattiglia EG. Polymer 1997;38:4469—76.

[20] Kelsey DR, Kiibler KS, Tutunjian PN. Polymer 2005;46:8937—46.

[21] Chin SJ, Cheng WH. J Anal Appl Pyrolysis 2000;56:131—43.

[22] Scott CE, Lazo NDB. In: Baker WE, Scott CE, Hu GH, editors. Reactive polymer blending. Hanser; 2001. p. 114—41.

[23] Harrats C, Groeninckx G. In: Ciardelli F, Penczek S, editors. Modification and blending of synthetic and natural macromolecules. Kluwer; 2004. p. 155—99.

[24] Loyens W, Groeninckx G. Polymer 2003;44:123—36.

[25] Lusinchi JM, Boutevin B, Torres N, Robin JJ. J Appl Polym Sci 2001;79:874.

[26] Yu ZZ, Lei M, Ou Y, Yang G. Polymer 2002;43:6993—7001.

[27] Pang YX, Jia DM, Hu HJ, Hourston DJ, Song M. Polymer 2000;41: 357—65.

[28] Orr CA, Cernohous JJ, Guegan P, Hirao A, Jeon HK, Macosko CW. Polymer 2001;42:8171—8.

[29] Coltelli MB, Savi S, Della Maggiore I, Liuzzo V, Aglietto M, Ciardelli F. Macromol Mater Eng 2004;289:400—12.

[30] Coltelli MB, Della Maggiore I, Savi S, Aglietto M, Ciardelli F. Polym Degrad Stab 2005;90:211—23; erratum 2006;91:987.

[31] Passaglia E, Marrucci M, Ruggeri G, Aglietto M. Gazz Chim Ital 1997;127:91.

[32] Fann DM, Huang SK, Lee JY. J Appl Polym Sci 1996;61:261—71.

[33] Awaja F, Pavel D. Eur Polym J 2005;41:1453—77.

[34] Kint DPR, Muñoz-Guerra S. Polym Int 2003;52:321.

[35] Coltelli MB, Bianchi S, Savi S, Liuzzo V, Aglietto M. Macromol Symp 2003;204:227—36.

[36] Otton J, Ratton S, Vasnev VA, Markova GD, Nametov KM, Bachmutov VI, et al. J Polym Sci Part A Polym Chem 1989;27:3535.

[37] Marèchal P, Legras R, Dekoninck JJ. Polym Sci Polym Phys 1995;33:1895.

[38] Aglietto M, Coltelli MB, Savi S, Lochiatto F, Ciardelli F, Giani M. J Mater Cycles Waste Manag 2004;6:13—9.